ELSEVIER

International Journal of Mass Spectrometry 178 (1998) 205–212

International Journal of Mass Spectrometry

Characterization of laser ablated species from a La–Ca–Mn–O target by angle- and time-resolved mass spectrometry

H.J. Dang, Z.H. Han, Z.G. Dai, Q.Z. Qin*

Laser Chemistry Institute, Fudan University, Shanghai 20043, People's Republic of China

Received 2 June 1998; accepted 15 July 1998

Abstract

The ablation of a $La_{1-x}Ca_xMnO_3$ (La–Ca–Mn–O) target under 532 and 355 nm laser irradiation has been investigated using an angle- and time-resolved quadrupole mass spectrometric technique. At laser fluence of 1.5 J/cm^2, we found the following ablated species: metal atoms La, Ca, Mn and metal ions La^+, Ca^+, Mn^+ as well as various metal oxides LaO, CaO, MnO, LaO_2, MnO_2, CaO_2. Small clusters such as Mn_2, La_2, Mn_2O and LaMnO were also observed. The measured time-of-flight (TOF) spectra are well fitted by a Maxwell-Boltzmann distribution with a stream velocity. The estimated kinetic energies of ablated metal ions are found to be in the range of 6–10 eV while those of neutral species range from 0.2 to 0.9 eV. The angular distributions of ablated species show that the ionic species are ejected within a cone shape plume characterized by a $\cos^n \theta$ function, while the angular distributions of the neutral species are much broader in comparison with the ionic species. The effect of laser radiation on possible ablation mechanisms are discussed. (Int J Mass Spectrom 178 (1998) 205–212) © 1998 Elsevier Science B.V.

Keywords: Laser ablation; Mass spectrometry; Angular distribution; La–Ca–Mn–O; Colossal magnetoresistance (CMR)

1. Introduction

As a powerful and universal deposition technique, pulsed laser deposition (PLD) received extensive experimental development for thin film fabrication. High Tc superconductor (HTSC) films such as Y–Ba–Cu–O [1] and oxide ceramic thin films such as $Sr_xBa_{1-x}TiO_3$ and $BaFe_{12}O_{19}$ [2] have been well prepared by the PLD method. A systematic effort in the characterization and modeling of various processes during PLD has been carried out by many authors [3,4]. Although the film quality strongly depends on the deposition conditions such as the substrate temperature, ambient pressure, and target-substrate distance, the composition of the laser ablated plume as well as the velocity and the spatial distributions of ablated species are very essential to the film deposition.

In recent years, the discovery of the negative and isotropic colossal magnetoresistance (CMR) in divalent metal doped lanthanide manganites has generated a hot topic because of their interesting physical properties and potential technological applications [5,6]. $La_{1-x}Ca_xMnO_3$ (La–Ca–Mn–O) is a typical example of CMR thin films which has been successfully fabricated by the PLD method [7,8]. So far, intensive studies on La–Ca–Mn–O system have been

* Corresponding author. E-mail: qzqin@fudan.ac.cn

PII S1387-3806(98)14094-0

carried out to optimize the film fabrication and to characterize the physical properties of the CMR film, but little is known about the plume composition and ablation mechanism underlying the PLD process. Recently, Lecceur et al. [9] employed optical emission spectrometric technique to study the oxidation of Mn atoms produced in the laser ablation of Mn, Mn_2O_3 and LaSrMnO. They confirmed the important role of oxidation reactions in deposition of a film with high quality. However, the detailed characterization of the ablated species have not been performed. Furthermore, optical emission technique can only be used to detect the excited ablated species and it provides a composition of ablated plume much simpler than the real case. Because the ablated plume consists of a major fraction of ablated species in the ground state, measurements of their composition, kinetic energy, and angular distributions are important in understanding the fundamental processes during PLD. Time-resolved mass spectrometry is another powerful technique for characterizing the laser ablated species in the ground state, and has been employed to study laser ablation of various materials such as HTSC [10], $CdWO_4$ [11], and Ta_2O_5 [12]. In this article, we present an angle- and time-resolved mass spectrometric characterization of the laser ablated plume from a La–Ca–Mn–O target at 532 and 355 nm. The mass distributions of the ablated species as well as their kinetic energies are determined and the angular distributions of the major ablated species are measured for the first time.

2. Experimental

The experimental apparatus used in this work has been described previously [12]. Briefly, a reaction chamber was pumped down to a base pressure of 10^{-6} Torr. The target pellet was mounted on a rotatable target holder at the center of the chamber. The La–Ca–Mn–O pellet was obtained by uniaxially compressing a mixture of stoichiometric amounts of La_2O_3, CaO and MnO_2(AR) for $La_{0.67}Ca_{0.33}MnO_3$ and calcined at 800°C for 5 h. The 355 and 532 nm laser beams were provided by the third and second harmonic frequencies of a Q-switched Nd-YAG laser (Quanta Ray GCR-190), and focused onto the target surface with an incident angle of 45° to the surface normal. The laser was operated with a pulse width of 6 ns and a repetition rate of 10 Hz. The diameter of the laser spot was about 1 mm and the laser intensity was measured by a power meter with a pyroelectric detector.

The ablated species were measured by a quadrupole mass spectrometer (QMS, ULVAC MSQ-400) housed in the detection chamber which can be moved around the reaction center in a range of 0°–90°. Two ion pumps were employed to evacuate the detection chamber down to $\sim 10^{-10}$ Torr. The flight distance of the ablated species was 18 cm from the target surface to the ionizer of QMS. The time-of-flight (TOF) spectra were recorded with a 20 MHz transient recorder which was interfaced to a 486 PC computer. The data acquisition was triggered synchronously with the laser pulses. The signal intensities or ablation yields of the ablated species are obtained by integrating the corresponding TOF spectra. Genuine ionic species were detected with the ionizer of QMS switched off. Both ionic and neutral species were recorded when the ionizer was switched on, in which the neutral ablated species were ionized by 70 eV electron impact. Taking into consideration of the drift time of the ion in the quadruple mass spectrometer, the measured TOF spectra should be calibrated by a drift time of $4.15M^{1/2}$ under our experimental conditions, where M is the relative mass of the ablated species.

3. Results and discussion

The experimental data obtained by time-resolved QMS technique show that the laser ablation of a La–Ca–Mn–O target at both 355 and 532 nm results in the generation of ionic and neutral metal atoms such as La, Ca, Mn, as well as metal oxides and small clusters. The TOF spectra of these ablated species have been measured at both wavelength. As their TOF profiles are similar in shape, we only present the TOF spectra of the Mn-containing species measured at 532

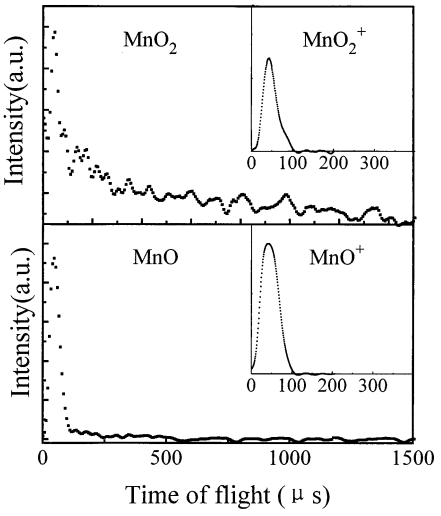

Fig. 1. The measured time-of-flight spectra of ionic and neutral species MnO (m/e 71) and MnO_2 (m/e 87) ablated from a La–Ca–Mn–O target by 532 nm with a laser fluence of 1.5 J/cm^2. The TOF spectra of ionic species are inserted in the right corner.

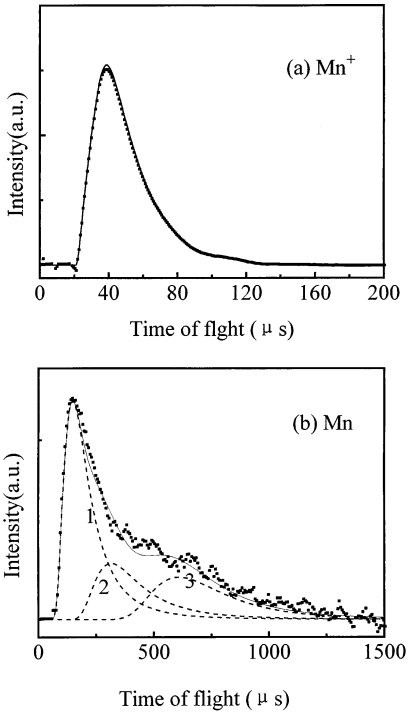

Fig. 2. The fittings of the time-of-flight spectra of Mn (m/e 55) measured with the ionizer switched off (a) and on (b). The broken lines are composites obtained from a three-component MB distribution. The solid line is the fitted curve.

nm for a laser fluence of 1.5 J/cm^2 in Figs. 1 and 2. It can be seen that the TOF spectra of genuine ions measured with the ionizer switched off are rather sharp and have a short flight time at the peak position, i.e. the ions possess high kinetic energies. But those measured with the ionizer switched on are more complicated. As shown in these figures, besides a fast component corresponding to the genuine ions, there appears a broad slow component following. It is reasonable to attribute the fast component to the genuine ions and the part of the neutral species formed by recombination of ions with electrons, while the slow component could be attributed to the neutral species formed through another path such as direct surface evaporation, or other parent molecules, which would be cracked in the ionizer of QMS.

In general, pulsed laser ablation of the metal oxides consists of three stages, including the laser-target interaction, the formation of the ablated plasma and the expansion of the ablated species [1]. Due to collisions among the ablated species, laser ablation of a solid surface usually produces a strongly forward ejection of species and behaves like a nozzle source. A supersonic expansion-type mechanism can be used to describe the pulsed laser ablated plume [13]. According to this model, the one-dimensional velocity distribution of ablated species can be fitted by a Maxwell-Boltzmann(MB) distribution modified by a stream velocity:

$$F(t) = ct^{-4}e^{-b_1t^{-2}+b_2t^{-1}} \quad (1)$$

where $b_1 = mL^2/2kT_s$, $b_2 = 2b_1u/L$, u is the stream velocity, L is the flight distance and Ts is a temperature parameter. When the detected ions originate from more than one parent components and each component can be fitted by a single-component MB distribution, their TOF spectra can be simulated by a multicomponent Maxwell-Boltzmann distribution with a stream velocity [14]:

$$F(t) = \sum_{i=1}^{p} Fi(t) = \sum_{i=1}^{p} c_it^{-4}e^{-b_{1i}t^{-2}+b_{2i}t^{-1}} \quad (2)$$

Table 1
A summary of the most probable velocity, $v_p(m/s)$, the stream velocity, $u(m/s)$, the kinetic energy, KE(eV), and the temperature parameter, Ts(K) for laser ablated species measured at 532 nm with a laser fluence of 1.5 J/cm^2

	Ionic species				Neutral species			
Species	v_p	u	KE	Ts	v_p	u	KE	Ts
Mn	4.7×10^3	2.0×10^3	6.3	2.2×10^4	1.2×10^3	2.3×10^2	0.43	2.9×10^3
MnO	4.3×10^3	1.7×10^3	6.9	3.3×10^4	1.2×10^3	/	0.56	2.8×10^3
MnO_2	4.4×10^3	1.6×10^3	8.7	3.3×10^4	1.2×10^3	/	0.67	2.9×10^3
Mn_2O	7.8×10^3	/	34	2.3×10^5		Undetected		
Mn_2	7.5×10^3	/	32	1.9×10^5		Undetected		
Ca	6.8×10^3	2.0×10^3	9.5	4.4×10^4	8.1×10^2	/	0.14	8.0×10^2
CaO	8.5×10^3	8.3×10^2	21	1.2×10^5	1.3×10^3	/	0.52	3.0×10^3
CaO_2	7.0×10^3	7.9×10^2	19	1.1×10^5	1.1×10^3	/	0.48	1.9×10^3
Ca_2	4.3×10^3	/	7.7	4.5×10^4	1.2×10^2	/	0.22	1.3×10^3
La	2.8×10^3	2.4×10^3	5.8	6.3×10^3	1.1×10^3	7.1×10^2	0.87	1.9×10^3
LaO	2.7×10^3	2.2×10^3	6.1	8.3×10^3	8.3×10^2	6.2×10^2	0.60	9.5×10^2
LaO_2	3.6×10^3	1.1×10^3	12	4.8×10^4	8.6×10^2	/	0.62	4.2×10^3
La_2O_3		Undetected			5.8×10^2	4.2×10^2	0.58	1.1×10^3
LaMnO	4.0×10^3	1480	18	7.1×10^4	6.2×10^2	1.0×10^2	0.42	2.4×10^3

where p is the number of parent component and c_i, b_{1i}, b_{2i} are the fitting parameters for each component. An example fitting is illustrated in Fig. 2 for the TOF spectra of Mn ($m/e = 55$). It can be seen that the TOF spectra of Mn measured with the ionizer switched off (a) and on (b) are well fitted by Eqs. (1) and (2), respectively. In order to give a clear illustration of the slow components, the fast component corresponding to the genuine Mn^+ ions has been excluded from the measured TOF spectrum in Fig. 2 (b). It can be seen that the TOF spectrum of Mn^+ ion (a) is fitted with Eq. (1) satisfactorily, giving a peak time $t_m = 38.2$ μs, corresponding to a kinetic energy of 6.3 eV and a stream velocity of 2.0×10^3 m/s. It means that Mn^+ ions might be directly ejected from the laser ablated plume. On the contrary, TOF spectrum of Mn atom (b) is characterized by a broader peak with a long tail, which can not be fitted by the Eq. (1), but a good fitting is obtained using a three-component MB distribution, i.e. the Eq. (2) with $p = 3$. The fitting result shows that the peak times for the three components are estimated to be 147, 315, and 640 μs, respectively, with stream velocities approach to zero. It implies that the first component could be attributed to the neutral Mn species with a kinetic energy of 0.43 eV, while the other components might be contributed from MnO and MnO_2, which can be cracked by 70 eV electron impact in the ionizer of QMS to produce Mn^+ ion signals. From the fitting results, the temperature parameters Ts are also estimated to be 2.2×10^4 and 2.9×10^3 K for genuine Mn^+ and Mn, respectively.

Similar simulations are carried out for the other ablated species, and the estimated most probable velocities(v_p), the stream velocities(u), the kinetic energies (KE) and the temperature parameters (Ts) are listed in Table 1. The following facts can be concluded given from the data in Table 1:

(1) For the ablated species with the same m/e value, the metal ions have the velocities in the range of 3×10^3 to 4.5×10^3 m/s, which corresponding to the kinetic energies from 6 to 10 eV, while those for neutral ablated species are much slower and their kinetic energies are found to be in the range of 0.2 to 0.9 eV.

(2) The temperature parameters Ts which may be related to the temperature of the near target region are estimated to be $(2 \sim 4) \times 10^4$ K for metal ions and $(2 \sim 4) \times 10^3$ K for neutrals. This implies that the neutral ablated species may come from a thermal equilibrium process such as thermal evaporation from the target surface, while the ionic ablated species may result from a nonthermal process in the ablated plasma.

(3) The ions and the fast components of neutrals possess a stream velocity as high as 2×10^3 m/s,

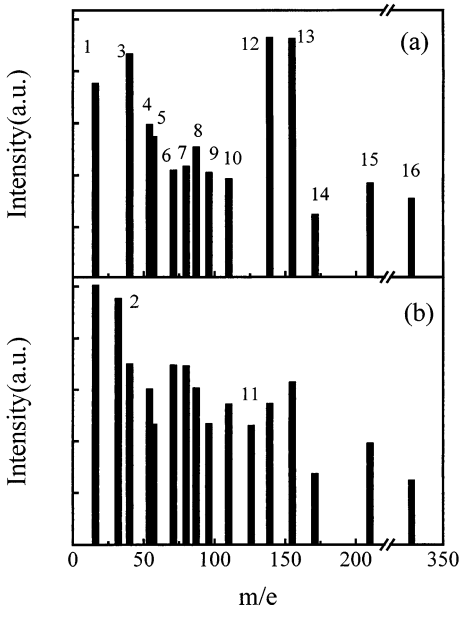

Fig. 3. Mass spectra of the ablated ions (a) and neutrals (b) from a La–Ca–Mn–O target under 355 nm pulsed laser irradiation at a laser fluence of 1.5 J/cm^2. 1—O, 2—O_2, 3—Ca, 4—Mn, 5—CaO, 6—MnO, 7—Ca_2, 8—MnO_2, 9—Ca_2O, 10—Mn_2, 11—Mn_2O, 12—La, 13—LaO, 14—LaO_2, 15—LaMnO, 16—La_2O_3.

while that of slow components for the neutrals are found to be one magnitude order slower. This result can also be explained by the different mechanism for the generation of the ionic and neutral ablated species as we mentioned above.

The mass distributions of the laser ablated species from a La–Ca–Mn–O target are obtained by integrating the measured TOF spectra. Fig. 3 presents the mass spectra of the laser ablated ionic (a) and neutral (b) species, respectively, at 335 nm with a laser fluence of 1.5 J/cm^2. It can be seen that besides metal ions and atoms, both ionic and neutral oxides such as MnO, MnO_2, CaO, LaO, LaO_2, and La_2O_3 are observed during laser ablation process. Furthermore, metal dimers and trimers Ca_2, Mn_2, as well as small clusters LaMnO and Mn_2O are also detected with low signal intensities. However, the mass distribution of ablated species strongly depends on the fluence. This is similar to that observed at 532 nm [15]. Furthermore, Fig. 4 shows the mass spectrum measured at a fluence of 0.3 J/cm^2, in which the major ablated

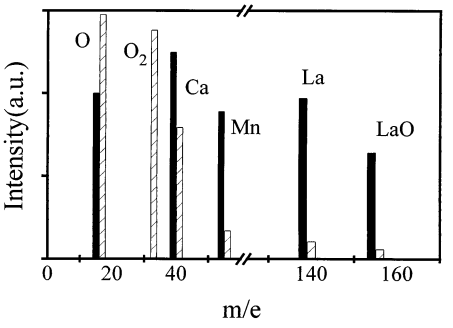

Fig. 4. Mass spectra of ablated species measured at a laser fluence of 0.3 J/cm^2 with the ionizer of QMS switched off (solid) and on (shadow).

species are Ca, Mn, La ions and neutral atoms, and LaO is the only metal oxide observed in comparable amount. Additionally, the signal intensities of MnO and CaO are very low and no other ablated species are detected. In fact, both the variety and the signal intensity of the ablated oxides increase with increasing the laser fluence. The laser fluence dependence of the signal intensities of the ablated ions Ca^+, Mn^+, and La^+ is illustrated in Fig. 5. It is seen that the ablation yields obviously increase with increasing laser fluence and a threshold seems to exist in the range from 0.3 to 0.6 J/cm^2 for different kinds of ablated species. The observation of more metal oxides and small clusters, such as LaMnO and Mn_2O at high laser fluence probably arises from secondary reactions between the ablated species in the ablated plasma.

The comparison between the laser ablation of the La–Ca–Mn–O target at the two wavelengths show that the laser wavelength makes no obvious differences in the mass distribution of the ablated species except that 355 nm radiation tends to generate more ionic species, and these ionic species possess higher kinetic energies than those for the 532 nm case. Table 2 lists the kinetic energies and the signal intensity ratios of ionic and neutral species for major ablated species measured at both wavelengths.

By comparing the relative intensities of LaO and MnO in the mass spectra, it is evident that intensity of LaO signal is strong even at low laser fluence while that of MnO is rather weak. This might be attributed to their different bond stability. The bond dissociation

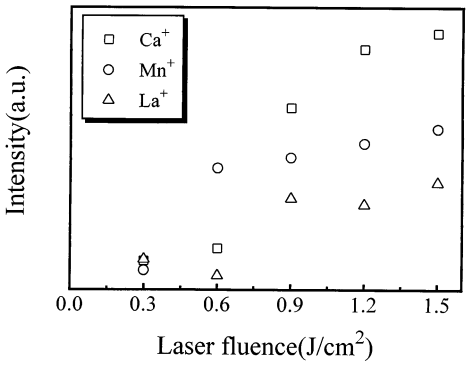

Fig. 5. The dependence of the signal intensity of ablated species on laser fluence.

energy of LaO is 8.29 eV which is higher than 4.3 eV of MnO [16]. Thus the MnO molecule dissociates readily and LaO does not. However, the relative signal intensity of MnO increases obviously at higher laser fluence. It might be because MnO is produced by both direct ablation and secondary reactions between Mn and O_2 in the laser induced plasma. The oxidation reaction of Mn

$$Mn + O_2 \rightarrow MnO + O \quad (3)$$

is endothermic (-1.0 ± 0.4 eV), so a thermal Mn atom cannot provide enough energy for the reaction in colliding with O_2. However, laser ablation produces a large amount of hyperthermal Mn^+ ions and Mn atoms which possess enough kinetic energy to overcome the energy barrier, and the oxidation reaction can take place during laser ablation of a La–Ca–Mn–O target.

The angular distributions of ablation species are of both fundamental and practical importance, due to their relevance to the film homogeneity and laser ablation dynamics. There is no report, however, on the determination of angular distributions of ablated species from a La–Ca–Mn–O target directly by a rotated QMS detecting at different angles. Fig. 6 presents the angular distributions of the ionic and neutral metal atoms Mn and La as examples. It is clear that the spatial distributions of both ionic and neutral atoms are strongly directed forward to the target surface normal. For a thermal evaporation process, it is well known that the particle ejection is moderately forward directed as a cos θ distribution (Knudsen law). However, a nonthermal process plays an important role in the laser ablation of a metal oxide target. It means that the ablated species in the laser induced plasma undergo a secondary ejection along the normal direction of the surface and create a high forward-peaked expansion. A model based on free-jet-expansion theory suggests that the angular distribution of ablated species can be described by a $\cos^n \theta$ distribution [17], where n is called sharpness parameter. In some ablation processes, the angular distributions of the ablated species can be expressed with a bicosine function $a \cos \theta + (1 - a)\cos^n \theta$. It implies that both thermal and nonthermal processes are important in the formation and expansion of the laser-induced plasma. The simulation results show that the data presented in Fig. 6 are well fitted by the following equations:

genuine Mn^+ ions $\cos^{60} \theta$

neutral Mn atoms $0.25 \cos \theta + 0.75 \cos^{40} \theta$

genuine La^+ ions $\cos^5 \theta$

neutral La atoms $0.1 \cos \theta + 0.9 \cos^5 \theta$

According to the above simulation results, it is evident that the sharp cone distributions of Mn^+ and La^+ ions follow essentially a $\cos^n \theta$, with an n value of 60 for Mn^+ ion, which is much greater than that for La^+ ion. It is interesting to note that the angular

Table 2
Laser wavelength effect on the kinetic energy of metal ions and signal intensity ratio of ion to neutral (M^+/M). Laser fluence = 1.5 J/cm^2 for both 355 and 532 nm.

	Kinetic energy of ions (eV)		Ion-neutral ratio (M^+/M)	
Species	532 nm	355 nm	532 nm	355 nm
Mn				
6.3	7.6	0.81	8.45	
La	5.8	7.3	3.17	9.28
Ca	9.5	20	1.40	1.59
LaO	6.1	7.5	6.74	42

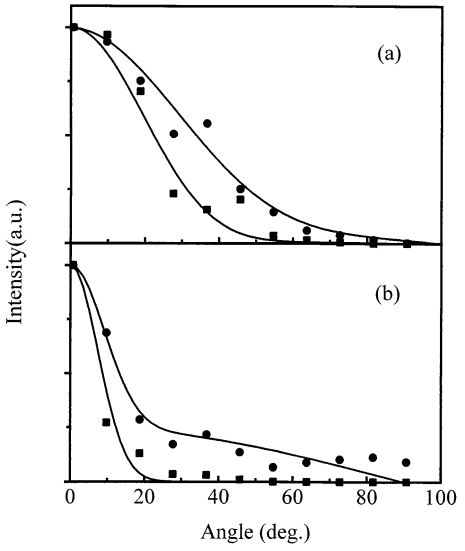

Fig. 6. Angular distributions of 532 nm laser ablated La (a) and Mn (b) species measured with ionizer switched off (squares) and on (circles). Solid lines are the fitted curves.

distributions of neutral ablated Mn and La atoms are well fitted by a bicosine function, implying that neutral species may originate from two different mechanisms. One part of neutral species are highly energetic, resulting from the ion–electron recombination and nonemitting decay of excited species. They have velocities comparable with those of the ions and expand into the vacuum together. By collision with each other, they are collimated along the surface normal and follow essentially a $\cos^n \theta$-type angular distribution. The other part of neutral species with lower velocities are produced by a thermal evaporation process which contribute to the $\cos \theta$ term. However, it has also been suggested that the ablated species at the relatively low-density wings of the expansion, as well as the leading and trailing edges of the pulse, will contribute to the broadened distribution, since these species will have suffered fewer collisions and thus have a more "effusive like" velocity distribution [17]. Since the angular distribution of ablated species in a laser ablation process depends on many other parameters such as the laser fluence, the ambient pressure, the surface properties, etc., the mechanism of laser ablation of La–Ca–Mn–O system is complicated and further investigation is needed.

4. Conclusions

We have successfully determined the mass, velocity and angular distributions of laser ablated species from a $La_{0.67}Ca_{0.33}MnO_3$ target at 532 and 355 nm using an angle- and time-resolved mass spectrometric technique. We found that apart from ionic and neutral metal atoms, a number of oxides including MnO, MnO_2, CaO, CaO_2, LaO, LaO_2, and La_2O_3 are produced at a high laser fluence. Small clusters Mn_2, Ca_2, Mn_2O and LaMnO are also observed. The kinetic energies of ionic species Mn^+, Ca^+, La^+ and LaO^+ measured at 532 nm are found to be 6.3, 9.5, 5.8, and 6.1 eV, respectively, and these ions possess higher kinetic energy for the 355 nm laser irradiation case. The laser fluence has a strong influence on both the variety and the intensity of the ablated species. The angular distributions of the ionic ablated species followed a $\cos^n \theta$ distribution while those of neutral ablated species can be described by a bicosine function $a \cos \theta + (1 - a) \cos^n \theta$. These results suggest that ionic ablated species are mainly produced via a nonthermal process such as photochemical and electron impact ionization processes in the plasma, while the neutral ablated species may result from both a thermal evaporation process and a nonthermal process. The observation of small clusters such as LaMnO provides evidence for the secondary reactions between ablated species in the laser plasma.

References

[1] D.H. Lowndes, D.B. Geohegan, A.A. Puretzky, D.P. Norton, C.M. Rouleau, Science 273 (1996) 898.
[2] D.B. Chrisey, J.S. Horwitz, P.C. Dorsey, Laser Focus World (May, 1995) 155.
[3] L.V. Zhigilei, B.J. Garrison, Appl. Phys. Lett. 71 (1997) 551.
[4] H.S. Kwok, Thin Solid Films 248 (1992) 277.
[5] S. Jin, T.H. Tiebel, M. McCormark, R.A. Fastnacht, R. Ramesh, L.H. Chen, Science 264 (1994) 413.
[6] H. Asano, J. Hayakawa, M. Matsui, Appl. Phys. Lett. 68 (1996) 3638.
[7] G.C. Xiong, S.C. Wu, D.S. Dai, B. Zhang, Z.X. Liu, G.J. Lian, Z.Z. Gan, Science in China (A) (Chinese Edition) 26 (1996) 722.

[8] G.C. Xiong, Q. Li, H.L. Ju, S.N. Mao, L. Senapati, X.X. Xi, R.L. Greene, T. Venkatesan, Appl. Phys. Lett. 66 (1995) 1427.
[9] P. Lecceur, A. Gupta, P.R. Duncompe, G.Q. Gong, Gang Xiao, J. Appl. Phys. 80 (1996) 513.
[10] G.C. Tyrrell, T.H. York, I.W. Boyd, Appl. Surf. Sci. 86 (1995) 50.
[11] K. Tanaka, T. Miyajima, N. Shirai, Q. Zhuang, R. Nakata, J. Appl. Phys. 77 (1995) 6581.
[12] Q.Z. Qin, Z.H. Han, H.J. Dang, J. Appl. Phys. 83 (1998) 6082.
[13] J.P. Zheng, Q.Y. Ying, S. Witanachichi, Z.Q. Huang, D.T. Shaw, H.S. Kwok, Appl. Phys. Lett. 54 (1989) 954.
[14] P.H. Lu, Q.Z. Qin, Science in China (A) (Chinese Edition) 23 (1993) 650.
[15] Dang Haijun, Han Zhenhui, Qin Qizong, Science in China (A) (Chinese Edition) (1998) in press.
[16] J.A. Dean, Lange's Handbook of Chemistry, 11th ed., McGraw-Hill, New York, 1973, pp. 3–124.
[17] R. Kelly, J. Chem. Phys. 92 (1990) 5047.